

Corneal primary aberrations compensation by oblique light incidence

Julian Espinosa

David Mas

Universidad de Alicante
Department Optica
Campus S Vicente
San Vicente del Raspeig
Alicante 03690
Spain

Henryk T. Kasprzak

Wroclaw University of Technology
Institute of Physics
Wybrzeze Wyspiankiego 27
Wroclaw 50-370
Poland

Abstract. The eye is not a centered system. The line of sight connects the fovea with the center of the pupil and is usually tilted in the temporal direction. Thus, off-axis optical aberrations, mainly coma and oblique astigmatism, are introduced at the fovea. Taberero et al. [*J. Opt. Soc. Am. A* **24**(10), 3274–3283 (2007)] showed that a horizontal tilt of the crystalline lens generates a horizontal coma aberration that is compensated by the oblique light incidence on the eye. Here we suggest that corneal astigmatism may also play a role in compensation of oblique aberrations, and we propose a simple model to analyze such a possibility. A theoretical Kooijman eye model with a slight (~ 0.6 D) with-the-rule astigmatism is analyzed. Light rays at different incidence angles to the optical axis are considered, and the corresponding point spread functions (PSFs) at the retina are calculated. A quality criterion is used to determine the incidence angle that provides the narrowest and highest PSF energy peak. We show that the best image is obtained for a tilted incidence angle compatible with mean values of the angle kappa. This suggests that angle kappa, lens tilt, and corneal astigmatism may combine to provide a passive compensation mechanism to minimize aberrations on the fovea. © 2009 Society of Photo-Optical Instrumentation Engineers. [DOI: 10.1117/1.3158996]

Keywords: astigmatism; angle kappa; ocular aberrations.

Paper 09039RR received Feb. 9, 2009; revised manuscript received May 12, 2009; accepted for publication May 12, 2009; published online Jul. 1, 2009.

1 Introduction

Visual perception is a complex task that occurs on two main stages. The first is optical image formation, which imposes the first physical limit to vision. The second is the capture and processing of the optical image by the retina and the brain. The optical part of the eye, with its biological surfaces that are constantly under development, is usually optically imperfect and suffers from asymmetries and aberrations. However, the eye's optics is also robust.¹ One of the most significant recent advancements in physiological optics was the recognition that different optical elements of the eye are balanced to produce an improved retinal image. Thus, corneal spherical aberration is balanced by the young crystalline lens.^{2–5} Other corneal aberrations like coma and astigmatism are also compensated by the internal optics of the eye,^{6,7} or by artificial lenses.⁸

Recent work has shown that, in addition to the balancing of the aberrations of different ocular components, the angle of incidence of light on the cornea could also play a role in aberration compensation. Kasprzak and Pierscionek⁹ propose a model of astigmatism in the cornea involving gravitational sag and the distribution in intraocular pressure. They give examples that, when rays enter the cornea at an appropriate angle, images with significantly reduced aberrations are produced.

Some aberrations may also come from misalignment between the eye's optical elements. The eye is not a centered system and its line of sight deviates from the optical axis. The angle between these axes is known as the kappa angle and is closely related to the distance between the pupil center and the corneal apex.¹ Taberero et al.⁷ studied the mechanism of compensation of ocular aberrations arising from oblique light incidence, and determined that the eye behaves as an aplanatic optical system when the actual shape factors of optical surfaces in the eye are combined with an appropriately tilted angle of incidence.

In these recent studies, little attention was paid to the compensation of residual astigmatism, since it is usually of low magnitude. Most ocular astigmatism is due to asymmetries in the corneal shape. The corneal astigmatism is usually partially compensated by the astigmatism of the internal optics of the eye, which provides approximately 0.5 D of the opposite sign.⁵ Nevertheless, typically there still remains some residual astigmatism that cannot be cancelled by the optics of the eye. Kelly et al.⁶ show that there is a consistent relationship between the magnitudes of the corneal and internal horizontal/vertical astigmatism aberration coefficients, and they suggest the existence of a fine-tuning mechanism that is feedback driven. However, this compensation mechanism only makes up for about 45% of astigmatism. Satterfield¹⁰ found that 63% of young adults between 20 and 30 years exhibited 0.25 D or

Address all correspondence to: David Mas, Dept. Optica, Universidad de Alicante, c/Alicante, s.n. 03690, San Vicente del Raspeig, Alicante Spain. Tel: 34 96 590 34 00 Ext. 2648; Fax: 34 96 590 34 64; E-mail: david.mas@ua.es

more of ocular astigmatism. Fledelius and Stubgaard¹¹ found that 46% of the total population had corneal astigmatism greater than 0.5 D, but only 4.7% of the population exhibited greater than 1.5 D of corneal astigmatism. It has also been determined that in young adults the axis of astigmatism is usually horizontal (with-the-rule). The genesis of the astigmatism and the reasons for this prevalence are not fully understood. Several possible factors have been suggested, including genetic factors, eyelid pressure, extraocular muscles tension, and visual feedback (see Ref. 12 for review).

Coma and astigmatism caused by oblique incidence share a common origin, since both aberrations appear when tilted rays enter an optical surface. Although Tabermer et al.⁷ state that crystalline lens horizontal tilt generates a horizontal coma aberration that is compensated by the kappa angle, they pay less attention to the possible effect of residual corneal astigmatism.

Our hypothesis is that the oblique incidence associated with the angle kappa may also play a role in compensating corneal astigmatism. Thus the angle kappa and foveal decentration play a double role in passively compensating both types of coma aberrations coming from the crystalline lens and residual corneal astigmatism.

In this work we have simulated a Kooijman theoretical eye with a slight with-the-rule astigmatism.¹³ Light rays at different angles of incidence are considered. Light patterns are propagated through the eye, and the location of the best image plane is determined. The results show that the best point spread function (PSF) is achieved when light is obliquely incident with a tilt that is compatible with mean values of the angle kappa, thus suggesting a mechanism of corneal passive compensation of corneal astigmatism.

2 Methods

2.1 Eye Model

The conical curves that are used for approximating ophthalmic surfaces in the eye can be represented in different forms. One of the most classic forms used to describe the refractive properties of the surfaces is:

$$z(x,y) = \frac{R_y}{(1+Q)} \left\{ 1 - \left[1 - \frac{(1+Q)}{R_y} \left(\frac{x^2}{R_x} + \frac{y^2}{R_y} \right) \right]^{1/2} \right\}, \quad (1)$$

where R_x , R_y , and Q are the two principal radii of curvature (in perpendicular axial planes) and the conic constant parameter, respectively, and x , y , and z are spatial coordinates, with the z axis being the optical axis.

We have used the parameters proposed by Kooijman¹³ to model the eye. Table 1 shows the values of the eye model. It is widely known that there is considerable intersubject variation of the astigmatism and its axis. Since our aim in this work is to suggest a possible compensation role of the corneal astigmatism, we have proposed a statistically typical young eye: for R_x we have taken values slightly greater than R_y to induce a slight with-the-rule astigmatism (~ 0.6 D).¹²

In the proposed model, the apices of the optical surfaces are aligned. The center of the entrance pupil is also aligned with the corneal apex, thus making a centered optical system. This is a deviation from real eyes, where the pupil and the

Table 1 Kooijman eye model parameters.

Surface	Anterior cornea	Posterior cornea	Anterior lens	Posterior lens
Radius (mm)	$R_x=7.9$ $R_y=7.8$	6.5	10.2	-6.0
Conic constant Q	-0.25	-0.25	-3.06	-1.0
	Cornea	Anterior chamber	Lens	Posterior chamber
Thickness (mm)	0.55	3.05	4.0	16.6
Refractive index	1.3771	1.3374	1.42	1.336

crystalline lens are usually displaced from the center of the cornea. Nevertheless, the model is simple and sufficiently accurate for our proposals.

2.2 Ray Tracing through the Eye

From the optical surfaces we have computed the optical path length of light passing through the cornea and crystalline lens using exact ray tracing. Let us consider a normalized ray vector \mathbf{v} incident on a surface. This vector is defined using direction cosines. Consider also a normalized vector \mathbf{q} that is normal to the surface at the incidence point.

$$\mathbf{v} = (v_x, v_y, v_z) = [\cos(\alpha), \cos(\beta), \cos(\gamma)], \quad (2)$$

$$\mathbf{q} = (q_x, q_y, q_z) = \left(\frac{\partial z}{\partial x}, \frac{\partial z}{\partial y}, 1 \right). \quad (3)$$

Let \mathbf{k} be the direction vector of the refracted ray:

$$\mathbf{k} = (k_x, k_y, k_z) = [\cos(\alpha'), \cos(\beta'), \cos(\gamma')].$$

The angles of incidence and refraction angles ε and ε' can be related using these vectors through

$$\mathbf{v} \cdot \mathbf{q} = \cos(\varepsilon),$$

$$\mathbf{k} \cdot \mathbf{q} = \cos(\varepsilon'),$$

$$\mathbf{v} \cdot \mathbf{k} = \cos(\varepsilon - \varepsilon'). \quad (4)$$

From the Snell law we can obtain the refracted ray \mathbf{k} at each point as:

$$\mathbf{k} = (k_x, k_y, k_z) = \left(\frac{n}{n'} \right) \mathbf{v} \pm \left[\cos(\varepsilon') \mp \frac{n}{n'} \cos(\varepsilon) \right] \mathbf{q}, \quad (5)$$

where the plus/minus signs stands for a convex or concave refracting surface.

With these equations we can calculate the optical path length from the anterior corneal surface to the posterior surface of the crystalline lens surface. To do so, we divide the calculation into five zones limited by the input and output

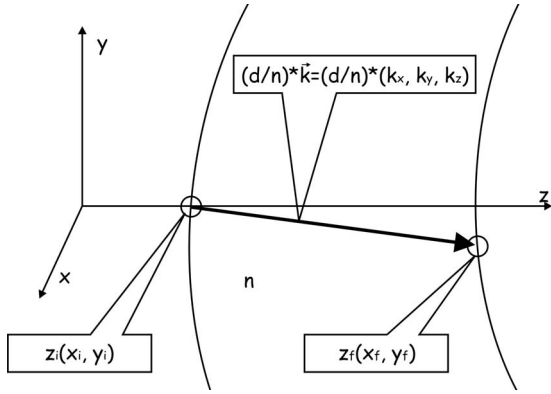


Fig. 1 Scheme for computing the optical path length.

planes of the different surfaces (the anterior and posterior surfaces of cornea and crystalline lens). The first input plane is defined perpendicular to the incident beam, while the final plane is situated immediately next to the posterior crystalline lens surface. It is perpendicular to the optical axis.

The first zone is defined from an input plane to the first corneal surface. Thus we compute the optical path length as the distance between that plane and the front corneal surface. The second zone goes from the anterior to the back corneal surface. Taking into account that surfaces are described by Eq. (1) and that the refracted ray $\mathbf{k} = [k_x, k_y, k_z]$ is known at each point of a surface, the optical path length d can be obtained by solving the equation:

$$z_i(x_i, y_i) + \left(\frac{d}{n}\right)_m k_{z,i} = z_f \left[x_i + \left(\frac{d}{n}\right)_m k_{x,i}, y_i + \left(\frac{d}{n}\right)_m k_{y,i} \right], \quad (6)$$

where the subindices i and f stand for the initial and final surface points, and subindex m refers to the medium between those surfaces. From here, the ray coordinates on the final surface are also obtained to compute the next refraction step.

Optical path lengths from the posterior corneal surface to the anterior crystalline lens surface, from the anterior to the posterior crystalline lens surfaces, and from the posterior crystalline lens surface to the exit plane are computed in the same way (see Fig. 1).

The total optical path length results from the sum of the computed optical paths for all the zones. If we depart from a uniformly sampled matrix, convergence of the rays causes the output optical path length to be evaluated at nonuniformly spaced coordinates (x, y) . A surface of the form $s = f(x, y)$ is therefore fitted to the total optical path length and then it is interpolated with a uniform grid. With these functions, we compute the phase transmittance of the optical part of the eye:

$$t(x, y) = \exp \left\{ \frac{i2\pi}{\lambda} [s(x, y)] \right\}, \quad (7)$$

and the propagated patterns are evaluated by means of a Fresnel propagation algorithm.¹⁴

2.3 Quality Criteria

The propagated patterns at different distances can be considered as generalized point spread functions (PSFs). The quality of each PSF is evaluated to determine the best image plane. Theoretically, the best image plane corresponds to that with the highest and narrowest PSF energy peak. These two parameters are evaluated, at the retinal plane for different incident light angles, through the maximum peak. The second moment of the energy distribution and the values of quality criteria are compared to determine the best coupling between oblique incidence and corneal astigmatism.

The calculation of the energy criterion is straightforward, since our calculation method¹⁴ provides the amplitude and phase of the light pattern at any desired distance. The second moment is obtained from the centroid position

$$M(x_i, y_j) = \sum_i \sum_j I(x_i, y_j) \cdot [(x_i - x_C)^2 + (y_j - y_C)^2], \quad (8)$$

where $I(x, y)$ is the light intensity value at each point of the plane of interest and (x_0, y_0) are the centroid coordinates defined as:

$$x_C = \frac{\sum_i \sum_j I(x_i, y_j) x_i}{\sum_i \sum_j I(x_i, y_j)}; \quad y_C = \frac{\sum_i \sum_j I(x_i, y_j) y_j}{\sum_i \sum_j I(x_i, y_j)}. \quad (9)$$

The second moment evaluates the width of the PSF, so that the lower the value of the second moment, the narrower and better the PSF is.

The use of two criteria may seem unnecessary when a perfect focus is achieved, but in the presence of astigmatism or other asymmetries, the two criteria may not reach their optimal value at the same incidence angle. Thus, we propose a merit function that takes into account both characteristics of the peak. The simplest function is:

$$C = \frac{\max[I(x, y)]}{M(x_0, y_0)}. \quad (10)$$

We evaluate the merit function for different incidence angles (α, β) at the best focus plane. Thus, the maximum values of the merit function $C(\alpha, \beta)$ will provide the best PSF.

To ensure that a decrease of astigmatism does not significantly increase other aberrations, we have also checked the variation of both astigmatism and coma aberration terms with the incidence angle. Refractive power maps provide a useful technique to analyze the wavefront aberrations. If an optical system is described in polar coordinates by a monochromatic wavefront $W(r, \theta)$, the estimate of the refractive power derived from the wavefront can be defined as¹⁵:

$$\hat{F}(r, \theta) = \left[W(r, \theta) + r \left(\frac{\partial W(r, \theta)}{\partial r} \right)^{-1} \right]^{-1} \cong \left(\frac{\partial W(r, \theta)}{\partial r} \right) r^{-1}. \quad (11)$$

It is possible to isolate the different aberration terms by decomposing the wavefront into Zernike polynomials, $Z_{n,m}(\rho, \theta) = N_{n,m} R_{n,m}(\rho) M_m(\theta)$, in polar coordinates (ρ, θ) ; n is the radial order, m the azimuthal frequency, and j the single index for the Zernike polynomial Z (see, e.g., Ref. 16). This decomposition can be expressed as

$$W(\rho, \theta) = \sum_{j=0}^{p-1} c_j Z_j(\rho, \theta), \quad (12)$$

$$j = \frac{1}{2}[n(n+2) + m]; \quad n = \left\lceil \frac{-3 + \sqrt{9 + 8j}}{2} \right\rceil;$$

$$m = 2j - n(n+2);$$

$$R_{n,m}(\rho) = \sum_{s=0}^{(n-|m|)/2} \frac{(-1)^s (n-s)!}{s![0.5(n+|m|)-s]![0.5(n-|m|)-s]!} \rho^{n-2s},$$

$$N_{n,m} = \left[\frac{2(n+1)}{1 + \delta_{m0}} \right]^{1/2}; \quad M_m(\theta) = \begin{cases} \cos(m\theta) & m \geq 0 \\ \sin(m\theta) & m < 0 \end{cases}, \quad (13)$$

where p is the number of terms in the expansion, c_j are the Zernike coefficients associated with their Zernike polynomial, and $\lceil \cdot \rceil$ denotes the ceiling (round-up) operator.

A more convenient form to analyze the polynomial in Eq. (12) involves rearranging the wavefront Zernike decomposition by grouping all the terms with the same radial degree and azimuthal frequency,¹⁷

$$W(\rho, \theta) = \sum_{j=0}^{p-1} g_j \rho^j M_m(\theta) = \sum_{j=0}^{p-1} g_j G_j(\rho, \theta). \quad (14)$$

From Eqs. (11) and (14), the estimate of the refractive power derived from the wavefront can be obtained as

$$\hat{F}(r, \theta) \cong r^{-1} \frac{\partial}{\partial r} \left[\sum_{j=3}^{p-1} g_j r^j M_m(\theta) \right] = \sum_{j=3}^{p-1} n g_j r^{j-2} M_m(\theta), \quad (15)$$

where $n g_j$ are directly related to the power vector components. For the case $n=2$ ($j=3$, $j=4$, and $j=5$), we obtain $2g_3 = -J_{45}$, $2g_4 = -M = -1/z_c$, and $2g_5 = -J_0$, i.e., the power vector components. If the reference sphere is subtracted, an aberration-free wavefront will be planar, i.e., the power map will be equal to zero. Hence, the PSF is better if the polynomial coefficients in Eq. (15) are lower.

3 Results

Using the values in Table 1, we have generated a Kooijman eye model. To introduce a slight corneal astigmatism, we have selected different values for the horizontal and vertical curvature radius, i.e., $R_x = 7.9$ mm; $R_y = 7.8$ mm. This difference causes a total with-the-rule ocular astigmatism of 0.6 D, similar to the mean values of astigmatism observed in the normal youth adult population. Pupil size has been limited to a natural pupil size of 4 mm in diameter. The ray incidence angle has been varied in both vertical and horizontal directions within the range $[-8$ deg, 8 deg] which corresponds to variations in the interval $[-82$ deg, 98 deg] for the direction angles α and β .

Figure 2 shows the values obtained for the quality parameter in the specified range. The maximum merit function value

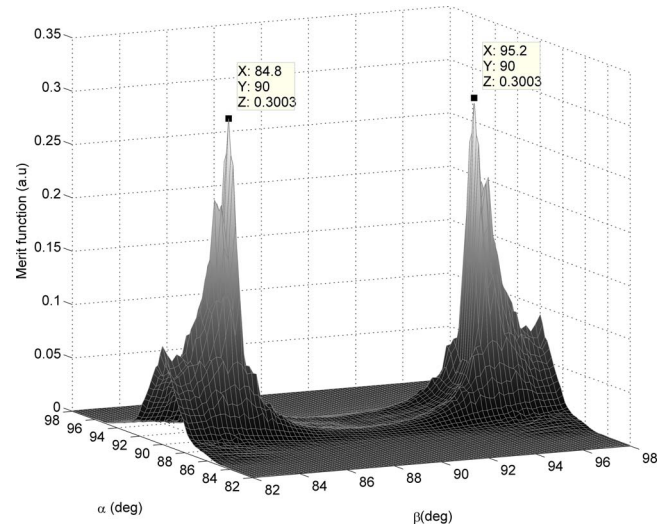


Fig. 2 Quality parameter for different incidence angles.

is reached for $(\alpha, \beta) = (84.8$ deg, 90 deg) and $(\alpha, \beta) = (95.2$ deg, 90 deg) equivalent to beams entering the cornea with incidence angles tilted at ± 5.2 deg in the horizontal direction. Different astigmatic corneas will provide maxima of the quality function at different incidence angles.

In Fig. 3, we show the values obtained for some of the power map coefficients described in Eq. (15). We have selected those that are more affected by an oblique incidence, since these will be the main contributors to the final quality of the PSF. Thus, we show absolute values of g_3 and g_5 , equivalent to J_{45} and J_0 , which describe astigmatism, and g_7 and g_8 that are directly related to vertical and horizontal coma, respectively. We have varied the incidence angle in the x direction, while the β angle has been fixed at 90 deg. In Fig. 3 we can see that $45/135$ astigmatism g_3 , and vertical coma g_7 , are not affected by the tilt of the ray, and their values are close to zero. On the other hand, the coefficient g_5 , related with $90/180$ astigmatism, decreases as the tilt angle approaches around 4.4 deg, as was predicted, but the coefficient for the vertical coma g_8 increases. Notice that the best image points

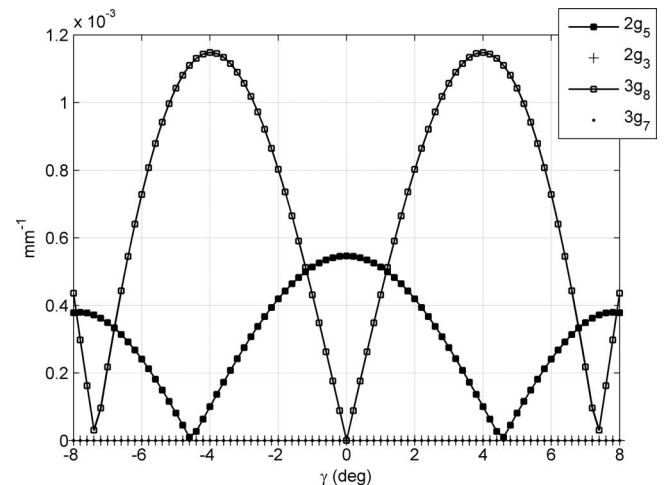


Fig. 3 Absolute astigmatism and coma Zernike coefficients.



Video 1 Retinal PSF at different incidence angles. Each frame has been normalized to its maximum value. Notice that the best image is obtained at $\gamma = \pm 5.2$ deg (MPG, 5.4 MG).
[URL: <http://dx.doi.org/10.1117/1.3158996.1>]

are obtained for incidence angles that provide a compromise between astigmatism compensation and coma increase.

Figure 2 provides a quantitative description of the passive compensation of oblique incident astigmatism by an astigmatic cornea. At first glance one can see that aberrations are canceled in two broad symmetric regions around $\gamma = \pm 5.8$ deg (note that $\gamma = 90 \text{ deg} - \alpha$ if $\beta = 90 \text{ deg}$) with maxima PSF peak values reached at $\gamma = \pm 5.2$ deg.

According to Fig. 3, the minimum of g_5 is reached at incidence angles of $\gamma = \pm 4.8$ deg. However, at these points the horizontal coma coefficient g_8 reaches values near its maxima. Thus, total cancellation of astigmatism implies an increase in the coma term. The merit function (Fig. 2) takes into account other contributions aside from only coma and astigmatism, and reaches its maximum values at $\gamma = \pm 5.2$ deg. At this point it seems that aberrations are conveniently balanced to give a PSF of reasonable quality.

To better understand the situation, in Video 1 we show the PSFs obtained for $\beta = 90$ deg and $\gamma \in [-8 \text{ deg}, 8 \text{ deg}]$. To allow better visualization, all the frames have been normalized to their maximum value, which is shown in the upper part. One can observe there that the PSF corresponding to $\gamma = \pm 5.2$ deg is better than the ones obtained for other incidence angles. We can also see the appearance of some coma in the PSF at this angle, as predicted in Fig. 3.

4 Discussion

We have shown that astigmatism induced by oblique incidence can compensate for the astigmatism of the cornea, although this tilt also induces comatic aberration. An apparent limitation of our calculations is the predicted symmetry of the optimal regions, which does not agree with the situation found in the real eye, where the foveal region is clearly determined. In the literature it is reported that peripheral astigmatism is minimum about one point of the nasal retina.^{18,19} Our results seem to agree with this finding, since we find a double mini-

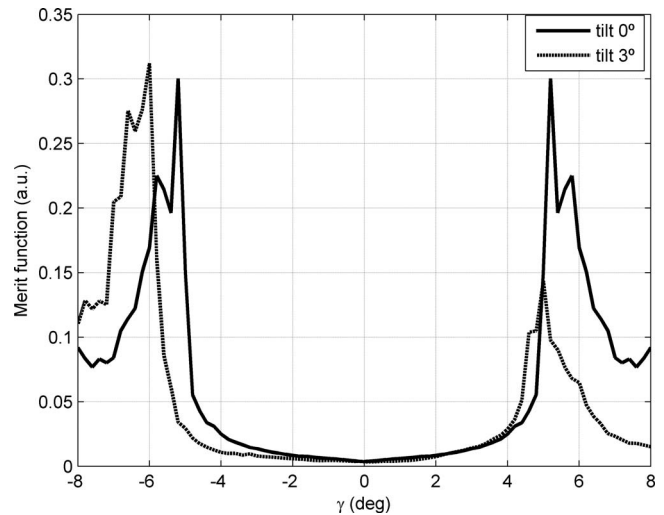


Fig. 4 Merit function on the x axis for the modeled eye with 0- and 3-deg crystalline lens tilt angles.

um in the astigmatism. Nevertheless, it has also been reported that in primates the fovea appears at the point where the best image is formed.²⁰ To our knowledge, this apparent contradiction means that, although astigmatism is one of the most important aberrations in the eye, higher order aberrations can play an important role in the definition of the best image point.

Here we have only considered a centered eye model and the effect of the cornea on astigmatism compensation. However, as explained in the introduction, crystalline lens tilt is known to play a fundamental role in coma compensation.⁷ Thus, introducing a tilted lens in our model will break the symmetry of the merit function by compensating the coma in one of the regions of interest.

In Fig. 4 we compare the merit function for angle $\beta = 90$ deg, i.e., tilting the incident beam only in the x direction, for the cases when there is either no tilt in the crystalline lens (continuous line) or a horizontal 3-deg crystalline lens tilt in the x direction (dotted line). In both cases, two peaks can be seen corresponding to a better PSF with oblique incidence, as compared to on-axis illumination. Furthermore, as we predicted, in the tilted crystalline lens case, the symmetry of the peaks is broken, with the peaks now occurring at $\gamma = -6.0$ deg and $\gamma = +5.2$ deg.

Figure 5 shows the absolute astigmatism and coma refractive power components for the modeled eye when modeled with a 3-deg crystalline lens tilt angle. We have included the results for the case with no crystalline lens tilt as a reference.

The tilted lens case (black and white circles) shows that astigmatism and coma components are now asymmetric about the axis. Furthermore, the maxima and minima have been displaced with respect to the no-tilt lens case. The minima of astigmatism are found in two points at both sides of the optical axis in partial agreement with Refs. 18 and 19, where they state the existence of a minimum only at the nasal side. Notice that in the region from $\gamma = -6$ deg to $\gamma = -7$ deg, there is a substantial decrease on both astigmatism and coma. Bearing in mind that the peak of the merit function shown in Fig. 4 is for an incidence angle $\gamma = -6$ deg, it seems that at this point

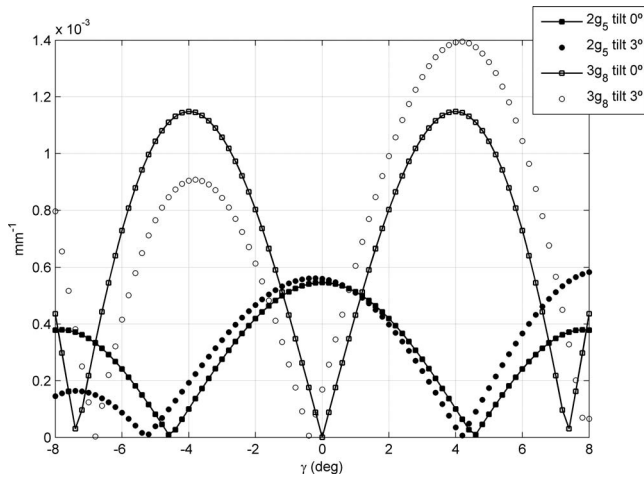


Fig. 5 Absolute astigmatism and coma refractive power components for the modeled eye with 0- and 3-deg crystalline lens tilt angles.

both aberrations are conveniently balanced to give a PSF of reasonable quality around the foveal region.²⁰ Notice also that according to the value of the merit function in Fig. 4, the best PSF is better than the one obtained without tilting the lens. This effect is due to the compensation of coma that was not achieved in the centered case.

Summarizing, the simulations presented in this work show that oblique incidence can compensate corneal astigmatism. We have modeled a simple theoretical eye with a small with-the-rule corneal astigmatism. Tilting of the rays may introduce a new aberration term with opposite sign to the existing one. We have proposed two simple quality criteria to evaluate the peak: maximum energy and second moment, which have been combined in a single merit function.

Although astigmatism is canceled, oblique incidence also induces coma in the final image. As noted by Tabernero et al. in Ref. 7, tilt of the crystalline lens may compensate this coma. Our simple model has shown that oblique incidence can passively compensate the effects of both corneal astigmatism and lens tilt on the foveal image, thus making the eye a robust optical system.

Normal values for the kappa angle are set between 4 and 8 deg with an average value of 5 deg. Results presented here locate the best image point within this range, which is in agreement with data from real eyes.

It is true that variability of eye parameters (asphericities, astigmatism, kappa angle, etc.) is considerable and the model here presented is necessarily limited. Kasprzak and Pierscionek⁴ suggested that gravitational corneal sag would also play some role in the compensation of aberrations by oblique incidence. It would be interesting to investigate correlations between lens tilt, corneal astigmatism, and angle kappa, as well as with other sources of aberrations in the eye,

but such studies are outside the scope of this communication and would require applications of more complex eye models.

Acknowledgments

David Mas acknowledges the support of the Generalitat Valenciana through the project BEST-2008-148. Henryk T. Kasprzak acknowledges the University of Alicante for its financial support through the project Senior 08/07.

References

1. P. Artal, A. Benito, and J. Tabernero, "The human eye is an example of robust optical design," *J. Vision* **6**, 1–7 (2006).
2. S. G. El Hage and F. Berny, "Contribution of the crystalline lens to the spherical aberration of the eye," *J. Opt. Soc. Am.* **63**, 205–211 (1973).
3. M. Millodot and J. Sivak, "Contribution of the cornea and lens to the spherical aberration of the eye," *Vision Res.* **19**, 685–687 (1979).
4. P. Artal and A. Guirao, "Contribution of cornea and crystalline lens to the aberrations of the human eye," *Opt. Lett.* **23**, 1713–1715 (1998).
5. P. Artal, A. Guirao, E. Berrio, and D. R. Williams, "Compensation of corneal aberrations by the internal optics in the human eye," *J. Vision* **1**, 1–8 (2001).
6. J. E. Kelly, T. Mihashi, and H. C. Howland, "Compensation of corneal horizontal/vertical astigmatism, lateral coma and spherical aberration by internal optics of the eye," *J. Vision* **4**, 262–271 (2004).
7. J. Tabernero, A. Benito, E. Alcón, and P. Artal, "Mechanism of compensation of aberrations in the human eye," *J. Opt. Soc. Am. A* **24**(10), 3274–3283 (2007).
8. S. Marcos, P. Rosales, L. Llorente, S. Barbero, and I. Jiménez-Alfaro, "Balance of corneal horizontal coma by internal optics in eyes with intraocular artificial lenses: evidence of a passive mechanism," *Vision Res.* **48**(1), 70–79 (2008).
9. H. Kasprzak and B. K. Pierscionek, "Modelling the gravitational sag of the cornea and the subsequent quality of the refracted image," *J. Mod. Opt.* **49**, 2153–2166 (2002).
10. D. S. Satterfield, "Prevalence and variation of astigmatism in a military population," *J. Am. Optom. Assoc.* **60**, 14–18 (1981).
11. H. C. Fledelius and M. Subgaard, "Changes in refraction and corneal curvature during growth and adult life, a cross sectional study," *Acta Ophthalmol.* **64**, 487–491 (1986).
12. S. A. Read, M. J. Collins, and L. G. Carney, "A review of astigmatism and its possible genesis," *Clin. Exp. Optom.* **90**, 5–19 (2007).
13. A. Kooijman, "Light distribution on the retina of a wide-angle theoretical eye," *J. Opt. Soc. Am.* **73**, 1544–1550 (1983).
14. D. Mas, J. Pérez, C. Hernández, C. Vázquez, J. J. Miret, and C. Illueca, "Fast numerical calculation of Fresnel patterns in convergent systems," *Opt. Commun.* **227**, 245–248 (2003).
15. D. R. Iskander, B. A. Davis, M. J. Collins, and R. Franklin, "Objective refraction from monochromatic wavefront aberrations via Zernike power polynomials," *Ophthalmic Physiol. Opt.* **27**, 245–255 (2007).
16. L. N. Thibos, R. A. Applegate, J. T. Schweigerling, and R. Webb, "Standards for reporting the optical aberrations of eyes," *J. Refract. Surg.* **18**, S652–S660 (2002).
17. J. Espinosa, D. Mas, J. Pérez, and C. Illueca, "Adaptive sampling in convergent beams," *Opt. Lett.* **33**, 1960–1962 (2008).
18. M. C. M. Dunne, G. P. Misson, E. K. White, and D. A. Barnes, "Peripheral astigmatic asymmetry and angle alpha," *Ophthalmic Physiol. Opt.* **13**, 303–305 (1996).
19. A. Seidemann, F. Schaeffel, A. Guirao, N. Lopez-Gil, and P. Artal, "Peripheral refractive errors in myopic, emmetropic, and hyperopic young subjects," *J. Opt. Soc. Am. A* **19**, 2363–2373 (2002).
20. A. D. Springer, "New role for the primate fovea: A retinal excavation determines photoreceptor deployment and shape," *Visual Neurosci.* **16**, 629–636 (1999).